State-Space Averaging (SSA) Revisited: On the Accuracy of SSA-Based Line-To-Output Frequency Responses of Switched DC-DC Converters

VIERA BIOLKOVA, ZDENEK KOLKA, DALIBOR BIOLEK
Depts. of Radio Electronics and Microelectronics, Brno University of Technology
Dept. of EE, University of Defence, Brno, Czech Republic
biolkova@feec.vutbr.cz, kolka@feec.vutbr.cz, dalibor.biolek@unob.cz

Abstract: The line-to-output (LTO) frequency response of switched DC-DC converter describes how the small-signal harmonic perturbation of the converted input DC voltage penetrates into the converter output, depending on the frequency of this perturbation. In the paper, the LTO frequency response conceived in this sense is faced with the LTO response, obtained by applying the well-known State-Space-Averaging (SSA) technique to switched converters, with the aim of determining the fundamental limitations of the SSA-approach. The general analysis is then applied to Buck-, Boost-, Buck-Boost-, and Cuk- type converters. It is shown that the accuracy of SSA outputs is related to the character of the state matrices of the converters.

Key-Words: switched DC-DC converter, averaging, SSA, spectrum, LTO frequency response

1 Introduction

Averaging belongs to the most popular tools for effective modeling and computer simulation of switched circuits with a view to DC-DC converters, both in the time and the frequency domains [1-22]. Instead of a complicated switched-level model of the converter, a simplified model is employed, which smoothes the switching effects and replaces the complicated waveforms by their low-frequency envelopes. The State-Space Averaging method (SSA) was published in 1977 [2], and circuit-oriented tools for simple building of the averaged models were subsequently designed, particularly the method of converter canonical models [3] and the method of PWM switch [4, 5]. Problems associated with the impact of ESR (Equivalent Series Resistances) modeling of filtering capacitors are also discussed in the last two references when the method of PWM switches can provide different results from those by the SSA approach. The final solution of the above problem is described in [6]. A special way of implementing the model of the PWM switch guarantees the same results as those of the SSA method. This procedure is then generalized in [7] for behavioral modeling of the actual influence of switch parameters, and another generalization is described in [8], providing automatic extraction of switch parameters from complex SPICE models of the transistor and the diode.

Since the average models enable a simple small-signal AC analysis, they play an irreplaceable role in the analysis of small-signal frequency responses of switched converters. However, since the averaging techniques represent a certain simplification of the original switched-level model, the question can arise whether such a simplification introduces errors in the AC analysis, with a negative impact, for instance, on the results of the stability testing of the switched regulator. Back in the original work [2], the accuracy of the SSA method is determined by a condition that the natural frequency of the filter inside the switched converter must be much lower than the switching frequency. An additional condition must be also fulfilled, namely that the frequency of the signal which modulates the switching duty ratio must be also substantially below the switching frequency [9], [10]. A statement is given in [11] that SSA provides exact results only for zero-frequency signals, and when this frequency approaches the switching frequency, the error becomes ill-defined. In fact, the switching frequency does not appear in the classical SSA method, but it represents an important real parameter of switched converter. In [12], two assumptions for a correct operation of the SSA method are defined: 1) The switching frequency is much higher than the highest natural frequency of the converters in each switching phase, and 2) the input of the converters in each switching phase must be time-independent or a slow time-varying variable in comparison with the switching frequency. In [13], the conditions for the justification of state-space averaging have been characterized as follows: a „small ripple" condition, a „linear ripple" approximation, and „the degree to which certain vector fields commute". As a consequence of these limitations, several modifications of the conventional averaging techniques have been developed, enabling, for example, an analysis of resonant-type converters [12, 13, 14] or predicting the switching instabilities in peak-current PWM converters [15].

The above facts can raise doubts whether the conventional SSA technique provides credible outputs of the analysis of frequency responses, particularly near and above the Nyquist frequency. When perturbing the input of the converter by a small-signal harmonic excitation with the frequency ω_i, there appears a rich spectrum at the converter output. If we consider the single spectral term at frequency ω_i, then the converter transfer function can be defined as a ratio of the phasor that represents this spectral term, to the phasor of the input signal. In this paper, we find an answer to the following question: Does the SSA method provide a frequency response, also known as the LTO (Line-To-Output) response, that precisely corresponds to the above transfer function?

The paper has the following structure: Section 2, which follows this Introduction, specifies the assumptions for the subsequent analysis, and introduces the model of switched converter. Based on the Fourier analysis, a structure of general equations of the converter is found, which enables numerical computation of the spectral terms of the output signal of the converter on the assumption of its harmonic excitation. Also, a connection between the conventional SSA equations and the above general equations is found, and an error term is identified which represents the disagreement between the output of the SSA method and the actual behavior of the converter. In Section 3, the results of numerical computations for Buck, Boost, Buck-Boost, and Cuk converters are presented, and connections between the SSA inaccuracies and the forms of the state matrices discussed.

2 Mathematical model

Let us consider a DC-DC converter consisting of linear passive elements and ideal switches that have r different configurations. Normally, $r = 2$ for converters operating in the continuous current mode (CCM), and $r = 3$ for converters operating in the discontinuous current mode (DCM).

Let us restrict the subsequent analysis to converters operating in CCM, where the switching instants are determined only by the external control signal, i.e. $r = 2$. In each switch configuration the converter represents a linear system

$$\frac{d}{dt}\mathbf{x} = \mathbf{A}_i\mathbf{x} + \mathbf{B}_i v, \, i = 1, 2, \tag{1}$$

where $\mathbf{x} \in \Re^n$ is the state vector, $\mathbf{A}_i \in \Re^{n \times n}$, $\mathbf{B}_i \in \Re^n$ are the converter state matrices and vectors, and v is the input voltage. Switch states periodically repeat with the period $T_s = 1/f_s = 2\pi/\omega_s$, where f_s (ω_s)

is the switching frequency.

Let the converter operate with a constant ratio of durations of switching phases T_1 and T_2, where $T_1+T_2 = T_s$, i.e. with a constant duty ratio $d = T_1/T_s$. Thus the results obtained by this analysis will be useful in assessing the applicability of the SSA method for converters operating with constant duty ratio and for the evaluation of accuracy of „line-to-output" responses.

With respect to the above assumptions, the converter can be regarded as a linear system with time-varying structure, having the state equations

$$\frac{d}{dt}\mathbf{x} = \mathbf{A}(t)\mathbf{x} + \mathbf{B}(t)v, \tag{2}$$

where $\mathbf{A}(t)$ and $\mathbf{B}(t)$ are periodic matrix (vector) functions with repeating period T_s.

With respect to periodicity, matrix $\mathbf{A}$ and vector $\mathbf{B}$ can be represented by the Fourier series:

$$\mathbf{A}(t) = \sum_{k=-\infty}^{+\infty}\mathbf{A}^{(k)}e^{jk\omega_s t}, \quad \mathbf{B}(t) = \sum_{k=-\infty}^{+\infty}\mathbf{B}^{(k)}e^{jk\omega_s t}. \tag{3}$$

In the case of two-state switching, where $\mathbf{A}_1$ and $\mathbf{B}_1$ correspond to the "ON" state of the active switch lasting for dT_s and $\mathbf{A}_2$ and $\mathbf{B}_2$ correspond to the "OFF" state lasting for $(1-d)T_s$, the spectral components $\mathbf{A}^{(k)}$ and $\mathbf{B}^{(k)}$ are given by the well-known formulae:

$$\mathbf{A}^{(0)} = d\mathbf{A}_1 + (1-d)\mathbf{A}_2 = \mathbf{A}_2 + d(\mathbf{A}_1 - \mathbf{A}_2),$$

$$\mathbf{A}^{(k)} = d\,\frac{\sin(k\pi d)}{k\pi d}e^{-jk\pi d}(\mathbf{A}_1 - \mathbf{A}_2), \, k\neq 0, \tag{4a}$$

$$\mathbf{B}^{(0)} = d\mathbf{B}_1 + (1-d)\mathbf{B}_2 = \mathbf{B}_2 + d(\mathbf{B}_1 - \mathbf{B}_2)$$

$$\mathbf{B}^{(k)} = d\,\frac{\sin(k\pi d)}{k\pi d}e^{-jk\pi d}(\mathbf{B}_1 - \mathbf{B}_2), \, k\neq 0. \tag{4b}$$

As system (2) is linear, a "one-sided" excitation of the converter can be considered in the form

$$v(t) = e^{j\omega_i t} \tag{5}$$

with frequency f_i (or $\omega_i=2\pi f_i$).

Then the spectrum of the state vector $\mathbf{x}$ of the converter in the steady state contains only components with combinational frequencies $k\omega_s+m\omega_i$, $k= \ldots -2, -1, 0, 1, 2, \ldots$, $m = -1, 0, 1$. The spectral term of the state vector on frequency $k\omega_s+m\omega_i$ will be denoted $\mathbf{x}^{(k,m)}$ or simply (k, m).
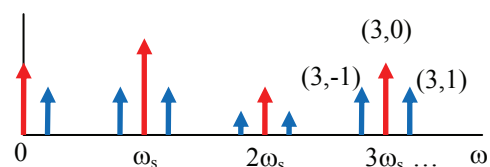

Fig. 1: Spectrum of state vector.

The Fourier series of the state vector can be written as

$$\mathbf{x}(t) = \sum_{k=-\infty}^{+\infty}\left[\mathbf{x}^{(k,0)}e^{jk\omega_s t} + \mathbf{x}^{(k,1)}e^{j(k\omega_s+\omega_i)t} + \mathbf{x}^{(k,-1)}e^{j(k\omega_s-\omega_i)t}\right] =$$

$$= \sum_{k=-\infty}^{+\infty}\left[\mathbf{x}^{(k,0)} + \mathbf{x}^{(k,1)}e^{j\omega_i t} + \mathbf{x}^{(k,-1)}e^{-j\omega_i t}\right]e^{jk\omega_s t}. \quad (6)$$

and its time-derivative will be

$$\frac{d}{dt}\mathbf{x}(t) = \sum_{k=-\infty}^{+\infty}[jk\omega_s\mathbf{x}^{(k,0)} + j(k\omega_s+\omega_i)\mathbf{x}^{(k,1)}e^{j\omega_i t} +$$

$$+ j(k\omega_s-\omega_i)\mathbf{x}^{(k,-1)}e^{-j\omega_i t}]e^{jk\omega_i t}. \quad (7)$$

With respect to (3), (5)-(7), state equation (2) can be rewritten to

$$\sum_{k=-\infty}^{+\infty}[jk\omega_s\mathbf{x}^{(k,0)} + j(k\omega_s+\omega_i)\mathbf{x}^{(k,1)}e^{j\omega_i t} +$$

$$+ j(k\omega_s-\omega_i)\mathbf{x}^{(k,-1)}e^{-j\omega_i t}]e^{jk\omega_i t} =$$

$$= \sum_{k=-\infty}^{+\infty}\mathbf{A}^{(k)}e^{jk\omega_s t}\sum_{k=-\infty}^{+\infty}\left[\mathbf{x}^{(k,0)} + \mathbf{x}^{(k,1)}e^{j\omega_i t} + \mathbf{x}^{(k,-1)}e^{-j\omega_i t}\right]e^{jk\omega_s t} +$$

$$+ \sum_{k=-\infty}^{+\infty}\mathbf{B}^{(k)}e^{jk\omega_s t}.e^{j\omega_i t}. \quad (8)$$

After a rearrangement we obtain

$$\sum_{k=-\infty}^{+\infty}[jk\omega_s\mathbf{x}^{(k,0)} + j(k\omega_s+\omega_i)\mathbf{x}^{(k,1)}e^{j\omega_i t} +$$

$$+ j(k\omega_s-\omega_i)\mathbf{x}^{(k,-1)}e^{-j\omega_i t}]e^{jk\omega_i t} =$$

$$= \sum_{k=-\infty}^{+\infty}\sum_{m=-\infty}^{+\infty}\mathbf{A}^{(k-m)}\left[\mathbf{x}^{(m,0)} + \mathbf{x}^{(m,1)}e^{j\omega_i t} + \mathbf{x}^{(m,-1)}e^{-j\omega_i t}\right]e^{jk\omega_s t} +$$

$$+ \sum_{k=-\infty}^{+\infty}\mathbf{B}^{(k)}e^{j(k\omega_s+\omega_i)t}, \quad (9)$$

representing an equality of the Fourier series of two signals. This means that individual spectral components with the corresponding frequencies must be equal.

Let us exclude cases where the spectral terms cross due to aliasing from further analyses. With respect to the fact that the spectra of matrix $\mathbf{A}$ and vector $\mathbf{B}$ contain only terms at multiples of ω_s, the energetic balance of (9) is formed separately by spectral components with the same index ω_i.

Therefore (9) can be divided into three equations: for components $(\bullet,+1)$

$$\sum_{k=-\infty}^{+\infty}\left[j(k\omega_s+\omega_i)\mathbf{x}^{(k,1)}\right]e^{j(k\omega_s+\omega_i)t} =$$

$$\sum_{k=-\infty}^{+\infty}\sum_{m=-\infty}^{+\infty}\mathbf{A}^{(k-m)}\mathbf{x}^{(m,1)}e^{j(k\omega_s+\omega_i)t} + \sum_{k=-\infty}^{+\infty}\mathbf{B}^{(k)}e^{j(k\omega_s+\omega_i)t}, \quad (10a)$$

for components $(\bullet,0)$

$$\sum_{k=-\infty}^{+\infty}\left[jk\omega_s\mathbf{x}^{(k,0)}\right]e^{jk\omega_s t} = \sum_{k=-\infty}^{+\infty}\sum_{m=-\infty}^{+\infty}\mathbf{A}^{(k-m)}\mathbf{x}^{(m,0)}e^{jk\omega_s t}, \quad (10b)$$

and for components $(\bullet,-1)$

$$\sum_{k=-\infty}^{+\infty}\left[j(k\omega_s-\omega_i)\mathbf{x}^{(k,-1)}\right]e^{j(k\omega_s-\omega_i)t} =$$

$$= \sum_{k=-\infty}^{+\infty}\sum_{m=-\infty}^{+\infty}\mathbf{A}^{(k-m)}\mathbf{x}^{(m,-1)}e^{j(k\omega_s-\omega_i)t}. \quad (10c)$$

For a fixed k, i.e. for a particular spectral component $(k,+1)$, the factor $e^{j(k\omega_s+\omega_i)t}$ in (10a) is reduced and we obtain a set of n infinite linear equations that follows from the equality of spectral component at frequency $k\omega_s+\omega_i$.

$$\sum_{m=-\infty}^{+\infty}\mathbf{A}^{(k-m)}\mathbf{x}^{(m,1)} - j(k\omega_s+\omega_i)\mathbf{x}^{(k,1)} = -\mathbf{B}^{(k)}. \quad (11)$$

Writing (11) for all spectral components leads to an infinite set of linear equations for an infinite number of unknowns $\mathbf{x}^{(k,1)}$. A fragment of the set is shown as (12). A similar procedure can be applied to (10b) for components $\mathbf{x}^{(k,0)}$, and to (10c) for components $\mathbf{x}^{(k,-1)}$. In contrast to (10a), both (10b) and (10c) lead to a homogenous set of equations as there is no input excitation at the particular frequencies.

It was proved in [23] that for passive circuits the infinite set of equations has one and only one solution, and any corresponding finite set of truncated equations have a unique solution. If the maximum frequency ω_i of the input signal is restricted, then the solution of the truncated set converges to the solution of the infinite set, i.e. for any chosen error there always exists a truncated set that approximates the solution of the infinite set with a lower error.

...					...		...
$\mathbf{A}^{(0)}$-$j(\omega_i$-$2\omega_s)\mathbf{E}$	$\mathbf{A}^{(-1)}$	$\mathbf{A}^{(-2)}$	$\mathbf{A}^{(-3)}$	$\mathbf{A}^{(-4)}$	$\mathbf{x}^{(-2,1)}$		$\mathbf{B}^{(-2)}$
$\mathbf{A}^{(1)}$	$\mathbf{A}^{(0)}$-$j(\omega_i$-$\omega_s)\mathbf{E}$	$\mathbf{A}^{(-1)}$	$\mathbf{A}^{(-2)}$	$\mathbf{A}^{(-3)}$	$\mathbf{x}^{(-1,1)}$		$\mathbf{B}^{(-1)}$
$\mathbf{A}^{(2)}$	$\mathbf{A}^{(1)}$	$\mathbf{A}^{(0)}$-$j\omega_i\mathbf{E}$	$\mathbf{A}^{(-1)}$	$\mathbf{A}^{(-2)}$	$\mathbf{x}^{(0,1)}$	$=-$	$\mathbf{B}^{(0)}$
$\mathbf{A}^{(3)}$	$\mathbf{A}^{(2)}$	$\mathbf{A}^{(1)}$	$\mathbf{A}^{(0)}$-$j(\omega_i$+$\omega_s)\mathbf{E}$	$\mathbf{A}^{(-1)}$	$\mathbf{x}^{(1,1)}$		$\mathbf{B}^{(1)}$
$\mathbf{A}^{(4)}$	$\mathbf{A}^{(3)}$	$\mathbf{A}^{(2)}$	$\mathbf{A}^{(1)}$	$\mathbf{A}^{(0)}$-$j(\omega_i$+$2\omega_s)\mathbf{E}$	$\mathbf{x}^{(2,1)}$		$\mathbf{B}^{(2)}$
...					...		...

(12)

It is obvious that a nonzero solution can be obtained only from (10a), which corresponds to the chosen input signal (5). Other spectral components will not be excited.

Assuming $k = 0$ in (11) and after a rearrangement we get

$$\left[\mathbf{A}^{(0)} - j\omega_i\mathbf{E}\right]\mathbf{x}^{(0,1)} + \sum_{\substack{m=-\infty \\ m\neq 0}}^{+\infty} \mathbf{A}^{(-m)}\mathbf{x}^{(m,1)} = -\mathbf{B}^{(0)}, \quad (13)$$

where $\mathbf{E}$ is the unity matrix.

Without the second term on the left-hand side, (13) represents the well-known state equation of the averaged model. Thus the second term represents an error factor that determines the difference between the averaged model and the reality.

The impact of the error term on the accuracy of the averaged model depends on the spectrum of matrix $\mathbf{A}$ and the spectral components $\mathbf{x}^{(m,1)}$, which represent ripple of the state vector around its average value. The spectrum of matrix $\mathbf{A}$ is determined by state matrices in the individual quasistable phases of the converter and by the duty ratio d. The influence of spectral components $\mathbf{x}^{(m,1)}$ decreases with increasing ratio of the switching frequency to the highest natural frequency of the converter.

Examining (12) and (13) one can find that:

- The error term in (13) exists even for $\omega_i = 0$ provided that $\mathbf{A}^{(k)}\neq\mathbf{0}$ for $k\neq0$. Harmonic components of the switching frequency $k\omega_s$ ($k\neq0$) are translated back to the DC component by the switching action, causing a difference between DC solution of the averaged model and reality.

- For $\omega_s\rightarrow\infty$, the amplitudes of all spectral components $\mathbf{x}^{(k,+1)}$ ($k\neq0$) of the state vector, which represent the ripple of state variables, vanish. It can be proved by rearranging (11) for $k\neq0$ to

$$\frac{\sum_{m=-\infty}^{+\infty} \mathbf{A}^{(k-m)}\mathbf{x}^{(m,1)}}{j(k\omega_s + \omega_i)} - \mathbf{x}^{(k,1)} = \frac{-\mathbf{B}^{(k)}}{j(k\omega_s + \omega_i)}. \quad (14)$$

As the spectral components of $\mathbf{A}$ are bounded and state variables $\mathbf{x}$ have finite energy, the sum on the left-hand side will be finite according to Parseval's theorem. For $\omega_s\rightarrow\infty$, we obtain a simple solution $\mathbf{x}^{(k,+1)} = 0$ for $k\neq0$. The only nonzero variable in (12) will be the component $\mathbf{x}^{(0,+1)}$. Equation (12) transforms into (13) with the zero error term on the left-hand side, i.e. into the averaged model.

The result confirms that in the case of negligible ripple of the state variables (i.e. for $\omega_s\rightarrow\infty$), the averaged model gives exact results.

The components of the error term in (13) can be computed numerically by truncating the original infinite set. Equation (13) is highlighted in (12). The magnitudes of the components of the generalized vector $\mathbf{x}^{(k,1)}$ quickly decrease with increasing k. The same holds for the spectral components of matrix $\mathbf{A}$ and vector $\mathbf{B}$. It is therefore possible to use a finite number of equations and to determine, with a certain error, the components of $\mathbf{x}^{(k,1)}$ by solving (12). It requires the knowledge of spectral components of matrices $\mathbf{A}$ and $\mathbf{B}$, and frequencies ω_i and ω_s.

Let us restrict the harmonic components $\mathbf{x}^{(k,1)}$ to a finite set, i.e. $k = -K, ...,0, ...,K.$, with K being a positive integer. For the converter with n accumulating elements (the state vector has n components), equation (12) represents a set of $(2K+1)n$ scalar linear equations. Numerical experiments show that starting from a certain value of K, a further increase in the number of harmonic components does not influence the component $(0,1)$. The number of harmonics is a trade-off between accuracy and the size of the resulting system of equations. If ω_M is the maximum frequency of interest of the input signal for examining LTO transfer functions, then

$$K > \left\lceil \frac{\omega_M}{\omega_s} \right\rceil. \quad (15)$$

Let us consider the truncated version of (12), where K has been chosen sufficiently high, such that the truncation error is negligible on the frequency interval of interest. Equations (12) can be rearranged as follows:

$$\begin{array}{|c|c|}\hline \mathbf{H}_{11} & \mathbf{H}_{12} \\ \hline \mathbf{H}_{21} & \mathbf{H}_{22} \\ \hline\end{array} \begin{array}{|c|} \widetilde{\mathbf{x}}^{(0,1)} \\ \widetilde{\mathbf{x}}^{(0,-K)} \\ \vdots \\ \widetilde{\mathbf{x}}^{(0,K)} \\ \end{array} = \begin{array}{|c|} \mathbf{G}_1 \\ \mathbf{G}_2 \\ \end{array}, \quad (16)$$

where $\widetilde{\mathbf{x}}$ is a truncated approximation of the exact solution, $\mathbf{H}_{11} = \mathbf{A}^{(0)} - j\omega_i\mathbf{E}$, $\mathbf{G}_1 = -\mathbf{B}^{(0)}$, $\mathbf{G}_2 = (-\mathbf{B}^{(-K)},...,-\mathbf{B}^{(-1)},-\mathbf{B}^{(1)},...,-\mathbf{B}^{(-K)})^T$, and $\mathbf{H}_{12}$ to $\mathbf{H}_{22}$ represent the remaining coefficients of the truncated set (12).

Then the SSA model can be written as

$$\mathbf{H}_{11}\mathbf{x}_A^{(0,1)} = \mathbf{G}_1, \quad (17)$$

where $\mathbf{x}_A$ is the averaged solution. The full model can be obtained by pivoting-out higher spectral components

$$(\mathbf{H}_{11} - \mathbf{H}_{12}\mathbf{H}_{22}^{-1}\mathbf{H}_{21})\widetilde{\mathbf{x}}^{(0,1)} = \mathbf{G}_1 - \mathbf{H}_{12}\mathbf{H}_{22}^{-1}\mathbf{G}_2. \quad (18)$$
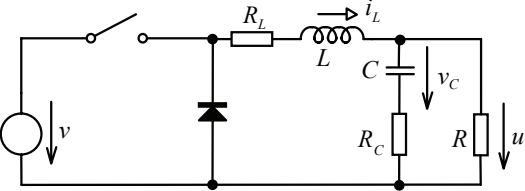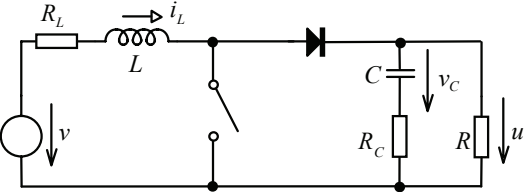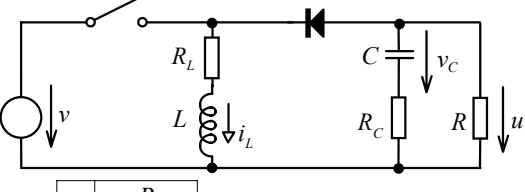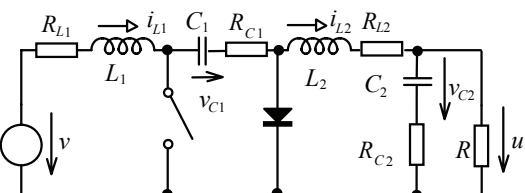
The difference between the state vectors for full and averaged model $\Delta\mathbf{x}_A^{(0,1)} = \widetilde{\mathbf{x}}^{(0,1)} - \mathbf{x}_A^{(0,1)}$ can be estimated from

$$\frac{\left\| \Delta \mathbf{x}_A^{(0,1)} \right\|}{\left\| \mathbf{x}_A^{(0,1)} \right\|} \le \text{cond}(\mathbf{H}_{11}) \left[\frac{\left\| \mathbf{H}_{12} \mathbf{H}_{22}^{-1} \mathbf{H}_{21} \right\|}{\left\| \mathbf{H}_{11} \right\|} + \frac{\left\| \mathbf{H}_{12} \mathbf{H}_{22}^{-1} \mathbf{G}_2 \right\|}{\left\| \mathbf{G}_1 \right\|} \right], \quad (19)$$

which follows from a general procedure for perturbed solution of linear equations [24].

The first term in brackets on the right-hand side

Table 1: Analyzed switched converters.

type	schematic, output description	state description
Buck	$\mathbf{C}_1 = \left[\, R_C \| R \;\middle|\; \dfrac{R}{R_C+R} \,\right],\; D_1 = 0$ $\mathbf{C}_2 = \left[\, R_C \| R \;\middle|\; \dfrac{R}{R_C+R} \,\right],\; D_2 = 0$	$\mathbf{A}_1 = \begin{bmatrix} -\dfrac{R_L + R_C\|R}{L} & -\dfrac{R}{L(R_C+R)} \\[2mm] \dfrac{R}{C(R_C+R)} & -\dfrac{1}{C(R_C+R)} \end{bmatrix},\; \mathbf{B}_1 = \begin{bmatrix} \dfrac{1}{L} \\[1mm] 0 \end{bmatrix}$ $\mathbf{A}_2 = \begin{bmatrix} -\dfrac{R_L + R_C\|R}{L} & -\dfrac{R}{L(R_C+R)} \\[2mm] \dfrac{R}{C(R_C+R)} & -\dfrac{1}{C(R_C+R)} \end{bmatrix},\; \mathbf{B}_2 = \mathbf{0}$
Boost	$\mathbf{C}_1 = \left[\, 0 \;\middle|\; \dfrac{R}{R_C+R} \,\right],\; D_1 = 0 \,,$ $\mathbf{C}_2 = \left[\, R_C \| R \;\middle|\; \dfrac{R}{R_C+R} \,\right],\; D_2 = 0$	$\mathbf{A}_1 = \begin{bmatrix} -\dfrac{R_L}{L} & 0 \\[2mm] 0 & -\dfrac{1}{C(R_C+R)} \end{bmatrix},\; \mathbf{B}_1 = \begin{bmatrix} \dfrac{1}{L} \\[1mm] 0 \end{bmatrix}$ $\mathbf{A}_2 = \begin{bmatrix} -\dfrac{R_L + R_C\|R}{L} & -\dfrac{R}{L(R_C+R)} \\[2mm] \dfrac{R}{C(R_C+R)} & -\dfrac{1}{C(R_C+R)} \end{bmatrix},\; \mathbf{B}_2 = \begin{bmatrix} \dfrac{1}{L} \\[1mm] 0 \end{bmatrix}$
Buck-Boost	$\mathbf{C}_1 = \left[\, 0 \;\middle|\; \dfrac{R}{R_C+R} \,\right],\; D_1 = 0$ $\mathbf{C}_2 = \left[\, -R_C \| R \;\middle|\; \dfrac{R}{R_C+R} \,\right],\; D_2 = 0$	$\mathbf{A}_1 = \begin{bmatrix} -\dfrac{R_L}{L} & 0 \\[2mm] 0 & -\dfrac{1}{C(R_C+R)} \end{bmatrix},\; \mathbf{B}_1 = \begin{bmatrix} \dfrac{1}{L} \\[1mm] 0 \end{bmatrix}$ $\mathbf{A}_2 = \begin{bmatrix} -\dfrac{R_L + R_C\|R}{L} & \dfrac{R}{L(R_C+R)} \\[2mm] -\dfrac{R}{C(R_C+R)} & -\dfrac{1}{C(R_C+R)} \end{bmatrix},\; \mathbf{B}_2 = \mathbf{0}$
Cuk	$\mathbf{C}_1 = \left[\, 0 \;\middle|\; R_{C2}\|R \;\middle|\; 0 \;\middle|\; \dfrac{R}{R_{C2}+R} \,\right],\; D_1 = 0$ $\mathbf{C}_2 = \left[\, 0 \;\middle|\; R_{C2}\|R \;\middle|\; 0 \;\middle|\; \dfrac{R}{R_{C2}+R} \,\right],\; D_2 = 0$	$\mathbf{A}_1 = \begin{bmatrix} -\dfrac{R_{L1}}{L_1} & 0 & 0 & 0 \\[2mm] 0 & -\dfrac{R\|R_{C2}+R_{L2}+R_{C1}}{L_2} & -\dfrac{1}{L_2} & -\dfrac{R}{L_2(R_{C2}+R)} \\[2mm] 0 & \dfrac{1}{C_1} & 0 & 0 \\[2mm] 0 & \dfrac{R}{C_2(R_{C2}+R)} & 0 & -\dfrac{1}{C_2(R_{C2}+R)} \end{bmatrix},\; \mathbf{B}_1 = \begin{bmatrix} \dfrac{1}{L_1} \\[1mm] 0 \\[1mm] 0 \\[1mm] 0 \end{bmatrix}$ $\mathbf{A}_2 = \begin{bmatrix} -\dfrac{R_{L1}+R_{C1}}{L_1} & 0 & -\dfrac{1}{L_1} & 0 \\[2mm] 0 & -\dfrac{R\|R_{C2}+R_{L2}}{L_2} & 0 & -\dfrac{R}{L_2(R_{C2}+R)} \\[2mm] \dfrac{1}{C_1} & 0 & 0 & 0 \\[2mm] 0 & \dfrac{R}{C_2(R_{C2}+R)} & 0 & -\dfrac{1}{C_2(R_{C2}+R)} \end{bmatrix},\; \mathbf{B}_2 = \begin{bmatrix} \dfrac{1}{L_1} \\[1mm] 0 \\[1mm] 0 \\[1mm] 0 \end{bmatrix}$

can be interpreted as an error caused by the excitation of higher harmonics from the component (0,1), and the second term represents the excitation due to the input signal.

3 Numerical experiments

In order to be able to compute small-signal transfer functions in a general case, it is necessary to complete (2) with the output equation to the full form of state description

$$u = \mathbf{C}(t)\mathbf{x} + D(t)v, \tag{20}$$

where u is the output voltage, $\mathbf{C}$ is a vector of dimension $(1, n)$, and D is a scalar.

Similar to the derivation of (10), we obtain the frequency domain form of (20)

$$\sum_{k=-\infty}^{+\infty} u^{(k,1)}\, e^{j(k\omega_s + \omega_i)t} = \sum_{k=-\infty}^{+\infty}\sum_{m=-\infty}^{+\infty} \mathbf{C}^{(k-m)}\mathbf{x}^{(m,1)}\, e^{j(k\omega_s + \omega_i)t} +$$

$$+ \sum_{k=-\infty}^{+\infty} D^{(k)} e^{j(k\omega_s + \omega_i)t} \ . \tag{21}$$

For the component $(k, 1)$ and a finite number of harmonic components we obtain finally

$$u^{(k,1)} = \sum_{m=-K}^{+K} \mathbf{C}^{(k-m)}\mathbf{x}^{(m,1)} + D^{(k)} \ . \tag{22}$$

The spectral components $\mathbf{C}^{(k-m)}$ and $D^{(k)}$ are given by formulae similar to (4).

The analysis has been implemented in Matlab for an arbitrary K and for an arbitrary number of switching phases. Boost, Buck, and Buck-Boost converters from Table 1 were analyzed using the following parameters that assure operation in the continuous-current mode:

$d = 0.25$, $f_s = 10$ kHz, $R = 60\ \Omega$, $C = 1$ mF, $L = 6$ mH, $R_C = 1\ \Omega$, $R_L = 3\ \Omega$.

The Cuk converter was analyzed using the following parameters:

$d = 0.25$, $f_s = 10$ kHz, $R = 60\ \Omega$, $C_1 = 1$ mF, $L_1 = 10$ mH, $R_{C1} = 1\ \Omega$, $R_{L1} = 5\ \Omega$, $L_2 = 10$ mH, $C_2 = 1$ mF, $R_{C2} = 1\ \Omega$, $R_{L2} = 5\ \Omega$.

The table shows all matrices and vectors of the complete state description. Figs. 2 and 3 show the results of AC analyses obtained by the numerical solution of (12) for $K = 10$.

A comparison of spectral component (0,1) with the LTO transfer functions generated by the SSA method shows a good agreement for the Buck and Boost converters in a wide frequency band, i.e. also above the Nyquist frequency $f_s/2 = 5$ kHz. But for the Buck-Boost and Cuk converters, a substantial difference occurs above the Nyquist frequency.
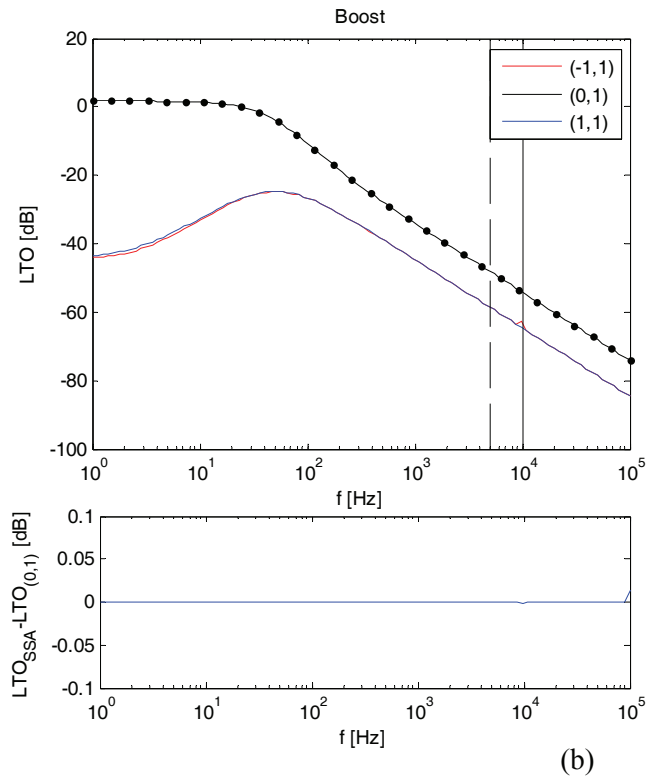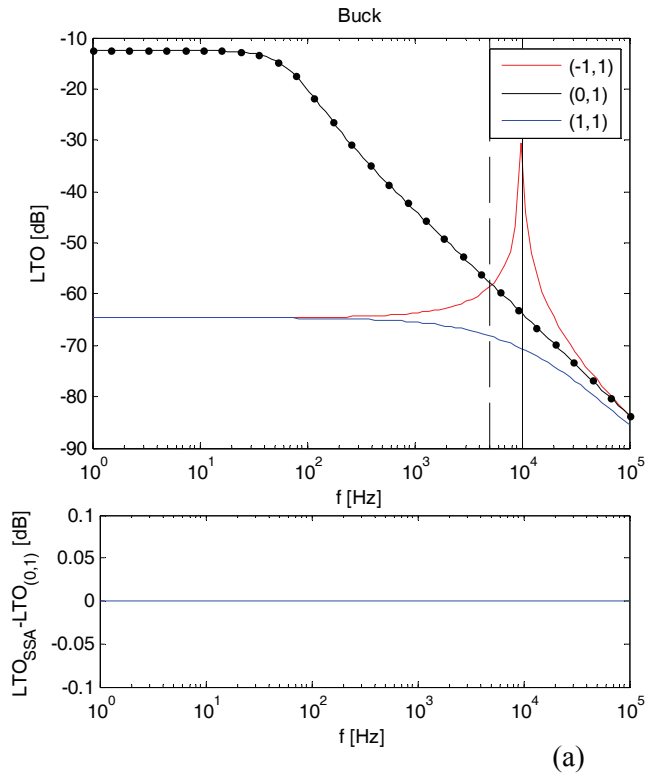

Fig. 2: Comparison of the LTO frequency response obtained from the averaged model (dots) with spectral components (-1,1), (0,1), and (1,1) for (a) Buck, (b) Boost converters. The vertical dashed line represents the 5 kHz Nyquist frequency and the full line represents the 10 kHz switching frequency.
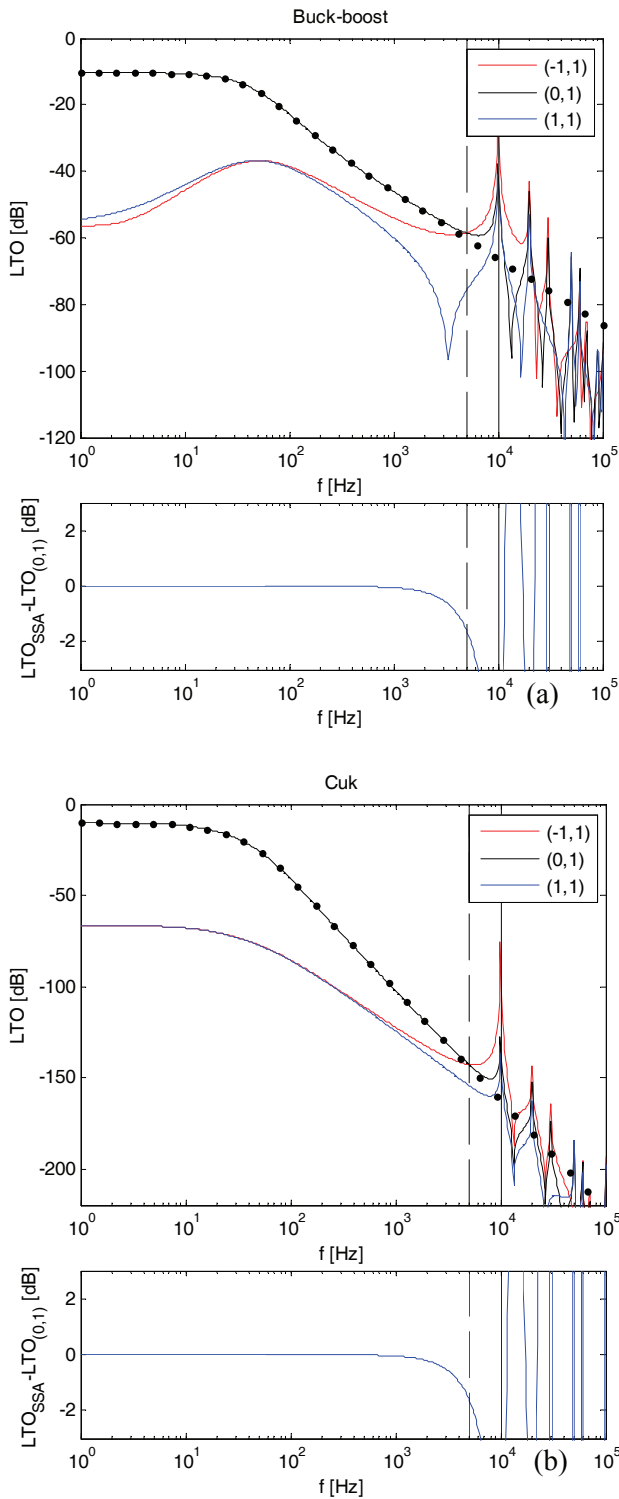
Fig. 3: Comparison of the LTO frequency response obtained from the averaged model (dots) with spectral components (-1,1), (0,1), and (1,1) for (a) Buck-Boost, (b) Cuk converters. The vertical dashed line represents the 5 kHz Nyquist frequency and the full line represents the 10 kHz switching frequency.

In the case of the Buck converter, the agreement between the results of the SSA method and the

frequency response (0,1) can be explained based on the form of state matrices $\mathbf{A}_1$ and $\mathbf{A}_2$ in Table 1. The matrices are the same. According to (4a) this means that all spectral components except for the DC component are zero: $\mathbf{A}^{(k)} = \mathbf{0}$, $k \neq 0$. It means that the error term on the left-hand side of (13) is zero, irrespective of the nonzero higher spectral components of the state vector, representing the ripple of circuit quantities. The equality of the two state matrices means that the SSA method gives correct results and provides an accurate AC analysis for all frequencies, i.e. also above the Nyquist frequency.

The spectrum of matrices $\mathbf{A}$ and $\mathbf{C}$ is rich for the Boost converter as the matrices are time-varying. Thus the frequency-conversion effects occur and there is energetic interaction between the spectral terms. As vector $\mathbf{B}$ is constant, the higher harmonics are not directly excited. Their nonzero magnitude results from the conversion of the (0,1) component. The higher harmonics cause the nonzero error term in (12), i.e. the difference between the component (0,1) and the LTO of the SSA model. However, their influence is negligible.

State equations of the Buck-Boost converter are similar to those of the Boost converter. As vector $\mathbf{B}$ is time-varying, the higher harmonics are directly excited in (13) and their magnitudes are comparable to the (0,1) component. The difference between (0,1) and LTO occurs even below the Nuquist frequency, as shown in Fig. 3a. A similar behavior can be observed in the Cuk converter. There is a substantial difference between (0,1) and LTO below the Nuquist frequency, see Fig. 3b.

Table 2 compares all four converters from the point of view of the interaction between the basic spectral component (0,1) and the higher components. The table shows both terms of (19) that quantify the influence of spectral conversion effects (matrix perturbation), and the external excitation (right-side perturbation) on the original SSA equations. The figures were obtained at the Nyquist frequency for the above values of network parameters.

Table 2: Influence of higher harmonics on component (0,1).

converter	$\|\Delta\mathbf{A}\|/\|\mathbf{A}\|$	$\|\Delta\mathbf{B}\|/\|\mathbf{B}\|$
Buck	0	0
Boost	$9.15*10^{-6}$	0
Buck-Boost	$9.15*10^{-6}$	$4.77*10^{-3}$
Cuk	$9.18*10^{-6}$	0

Let us consider an idealized Boost converter with lossless accumulation elements ($R_C = 0$, $R_L = 0$).

Then its SSA model is simple enough to be solved symbolically. The LTO transfer function in CCM is then

$$K_{LTO,BT} = \frac{1-d}{s^2 LC + sL/R + (1-d)^2} \ . \qquad (23)$$

The converter works in CCM if the accumulation inductance L is greater than the minimum value

$$L_{min} = \frac{d(1-d)^2 R}{2 f_S} \ . \qquad (24)$$

The formula holds for a practical case when the output voltage ripple is negligible. For $L = L_{min}$ the minimum inductor current is 0, i.e. the current ripple is the maximum possible for CCM. Thus the higher harmonics, which cause the SSA model error, will be maximum.

Let us fix the inductance at the value $L = L_{min}$. The LTO transfer function will be

$$\widetilde{K}_{LTO,BT} = \frac{1}{1-d} \frac{1}{s_N^2 \left(\dfrac{RCf_S}{d} \right) 2\pi^2 d^2 + s_N \pi d + 1} \ , \qquad (25)$$

where $s_N = s/(2\pi f_S)$ is the normalized complex frequency. The term in brackets in the denominator represents the reciprocal value of the output ripple for ideal capacitor, i.e. for $R_C = 0$ [9]

$$\frac{\Delta u}{u} = k_r = \frac{d}{RCf_S} \ . \qquad (26)$$

At the boundary of CCM, the LTO transfer function of simplified converter depends only on the duty ratio d and the required output ripple.

A similar procedure can be applied to the Buck-Boost converter. The LTO transfer function of the lossless converter is

$$K_{LTO,BB} = \frac{-d(1-d)}{s^2 LC + sL/R + (1-d)^2} \ . \qquad (27)$$

The minimum inductance for the CCM operation is [9]

$$L_{min} = \frac{(1-d)^2 R}{2 f_S} \ , \qquad (28)$$

which leads to

$$\widetilde{K}_{LTO,BB} = \frac{-d}{1-d} \frac{1}{s_N^2 \left(\dfrac{RCf_S}{d} \right) 2\pi^2 d + s_N \pi + 1} \ . \qquad (29)$$

Formula (26) for the output ripple also holds for the Buck-Boost converter.

Figs. 4 and 5 show the results of numerical simulation for the Boost and Buck-Boost converters at the boundary between CCM and DCM in order to evaluate the worst-case error of the SSA method.

The accumulation inductance was set according to (24) and (28) for three values of the duty ratio d. The capacitor value was computed for $k_r = 0.01$. Plot (a) shows the difference between SSA and full-model LTO responses in decibels for lossless converter. Plots (b) and (c) show the results for capacitor normalized ESR being $R_C/R = 0.01$, and plot (c) for inductor normalized ESR being $R_L/L = 0.5 \ 10^{-3}$. In cases (b) and (c), the inductance was adjusted numerically, ensuring operation at the CCM boundary.
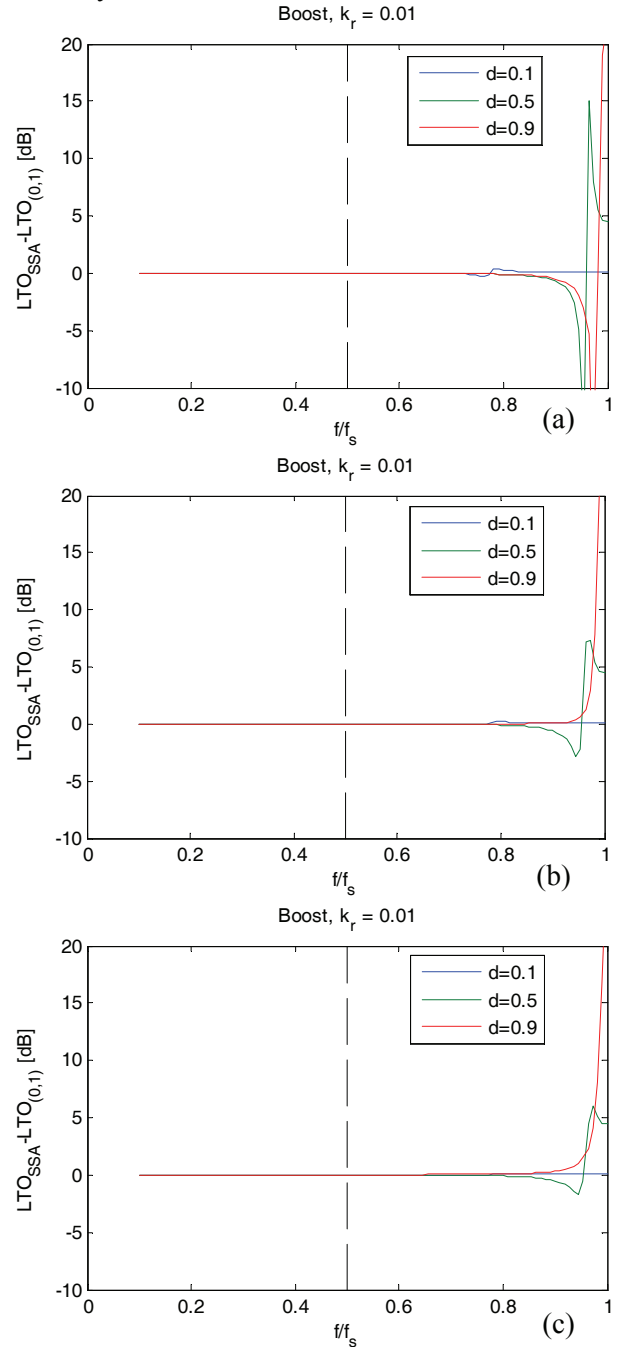

Fig. 4: Error of SSA LTO frequency response for Boost converter at CCM boundary, (a) ideal, (b) with R_C, (c) with R_C and R_L. The vertical dashed line represents the 5 kHz Nyquist frequency.
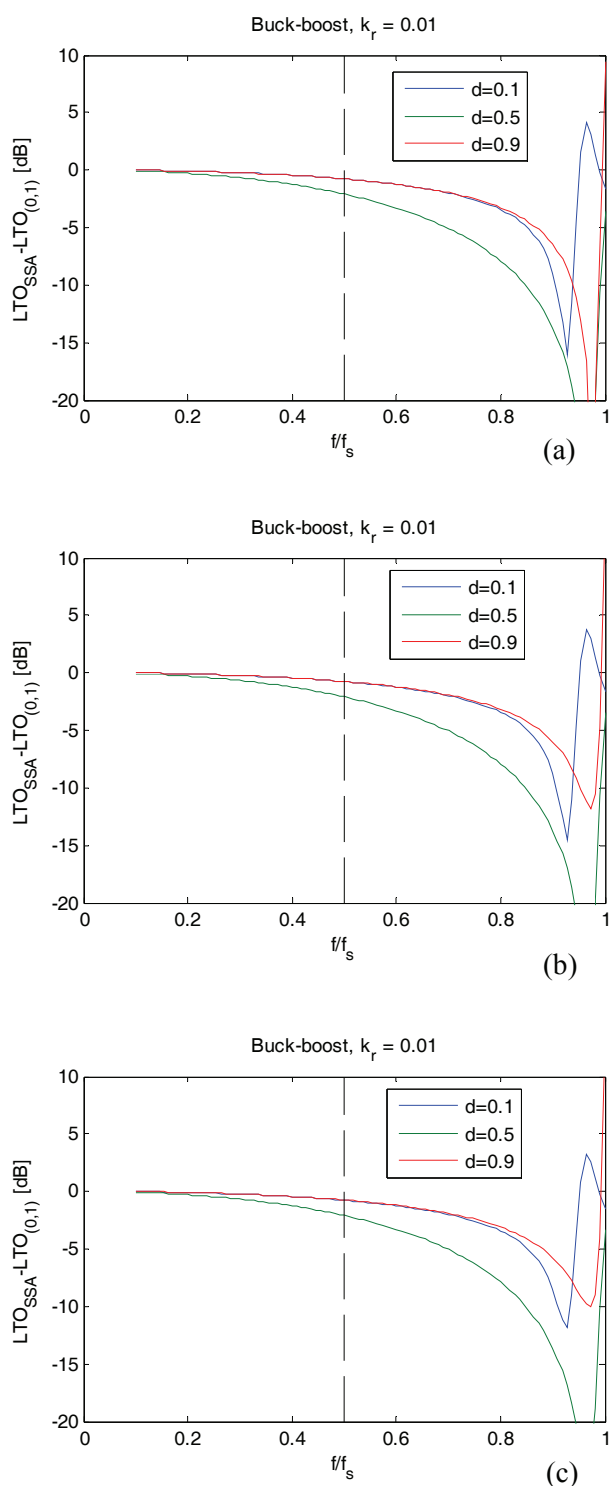
Fig. 5: Error of SSA LTO frequency response for Buck-Boost converter at CCM boundary, (a) ideal, (b) with R_C, (c) with R_C and R_L. The vertical dashed line represents the 5 kHz Nyquist frequency.

Fig. 4 shows that the error is negligible for the Boost converter approximately up to 0.8 of the switching frequency. The analysis of Buck-Boost converter in Fig. 5 exhibits a substantial error even below the Nyquist frequency.

4 Conclusions

The paper shows that:

(a) There is a simple numerical method for determining an arbitrary number of spectral components of the response of a switched converter excited by a single-tone input signal. It allows performing a generalized AC analysis of the converter.

(b) The classical SSA equations can be seen as a simplified case of the general equation of switching converter that determines the response to the harmonic input signal in the frequency domain.

(c) The difference between SSA model and actual converter behavior is given by the error term that depends on state matrices in quasistable switching phases and on higher spectral components of state variables.

(d) The SSA method provides the most accurate results for the Buck converter, whose state matrices A_1 and A_2 are identical in both switching phases. The results of AC analysis are valid in a broad frequency band, i.e. also above the Nuquist frequency. On the other hand, inaccuracies occur even below the Nyquist frequency for the Buck-Boost converter.

References:

[1] Middlebrook, R.D., Ćuk, S. A general unified approach to modeling switching-converter power stages. *Int. Journal of Electronics*, Vol. 42, No. 6, 1977, pp. 512-550.

[2] Wester, G.W., Middlebrook, R.D. Low-frequency characterization of switched dc-dc converters. *IEEE Trans. On Aerospace and Electronic Systems*, Vol. AES-9, No. 3, 1973, pp. 376-385.

[3] Middlebrook, R.D. Small-signal modelling of pulse-width modulated switched-mode power converters. *Proceedings of the IEEE*, Vol. 76, No. 4, 1988, pp.343-354.

[4] Tymerski, R.P.E. et al. Nonlinear modeling of the PWM switch. *IEEE Trans. on Power Electronics*, Vol. 4, No. 2, 1989, pp. 225-233.

[5] Vorpérian, V. Simplified analysis of PWM converters using the model of the PWM switch: Parts I and II. *IEEE Trans. on Aerospace Electronic Systems*, Vol. 26, No. 3, 1990, pp. 490-505.

[6] Dijk, E., Spruijt, J.N., Sullivan, M.O., Klaassens, J.B. PWM-switch modeling of DC-DC converters. *IEEE Trans. on Power Electronics*, Vol. 10, No. 6, 1995, pp. 659-664.

[7] Biolek, D., Biolkova, V., Kolka, Z. SPICE modeling of switched DC-DC converters via generalized model of PWM switch. In Proc. of IEEE Radioelektronika, 2007, pp. 1-4.

[8] Biolek, D., Biolkova, V., Kolka, Z. Averaged Modeling of Switched DC-DC Converters based on Spice Models of Semiconductor Switches. In Proc. of CSECS'08, December 2008, pp. 162-167.

[9] Erickson, R. W. *Fundamentals of Power Electronics*. Cluwer Academic Publishers, 2004.

[10] Basso, C.P. *Switch-mode power* supply *SPICE cookbook*. McGraw-Hill, 2001.

[11] Bina, M.T., Bhat, K.S. Averaging technique for the modelling of STATCOM and active filters. *IEEE Trans. On Power Electronics*, Vol. 23, No. 2, 2008, pp. 723-734.

[12] Xu, J., Lee, C.Q. A unified averaging technique for the modelling of quasi-resonant converters. *IEEE Trans. On Power Electronics*, Vol. 13, No. 3, 1998, pp. 556-563.

[13] Sanders, S.R., Noworolski, J.M., Liu, X.Z., Verghese, G.C. Generalized averaging method for power conversion circuits. *IEEE PESC'90*, Rec., 1990, pp. 333-340.

[14] Noworolski, J.M., Sanders, S.R. Generalized in-place circuit averaging. *IEEE PESC'91*, Rec., 1991, pp. 445-450.

[15] Sun, J., Choi, B. Averaged modelling and switching instability prediction for peak-current control. *IEEE PESC'05*, Rec., 2005, pp. 2764-2770.

[16] Biolkova, V., Kolka, Z., Biolek, D. On the Validity of SSA-based Models of DC-DC Converters. Proc. of the CSECS'09, 8th WSEAS Int. Conference on Circuits, Systems,

Electronics, Control&Signal Processing, Tenerife, Spain, December 2009, pp. 202-207.

[17] Biolek, D., Biolková, V., Kolka, Z. AC Analysis of Idealized Switched-Capacitor Circuits in Spice-Compatible Programs. In Proc. of CSCC07, The 11th WSEAS Int. Conf. on Circuits, Crete, 2007, pp. 222-226.

[18] Biolek, D., Biolkova, V., Kolka, Z. AC analysis of real circuits with external switching in PSpice. In Proc. CSCC08, the 12th WSEAS Int. Conf. on Circuits, Heraklion, Greece, July 22-24, 2008, pp. 193-196.

[19] Biolek, D., Biolková, V., Kolka, Z. Analysis of Switching Effects in DC-DC Converters via Bias Point Computation. In Proc. of ECCTD07, The European Conference on Circuit Theory and Design, 2007, pp. 1006-1009.

[20] Biolek, D., Biolková, V., Dobeš, J. Modeling of switched DC-DC converters by mixed s-z description. In Proc. of the IEEE Int. Symp. on Circuits and Systems, ISCAS2006, Greece, Kos, 2006, pp. 831 – 834.

[21] Biolek, D., Biolková, V., Kolka, Z. PSPICE modelling of Buck Converter by means of GFTs. *WSEAS Trans. on Electronics*, 2006, Vol. 3, No. 2, pp. 93 - 96.

[22] Jaroš, M., Kadlec, J., Biolek, D. Unconventional simulation taskas in OrCAD PSpice via Simulation Manager. In Proc. of CSCC08, the 12th WSEAS Int. Conf. on Circuits, Heraklion, Greece, July 22-24, 2008, pp. 189-192.

[23] Sandberg, I. On Truncation Techniques in the Approximate Analysis of Periodically Time-Varying Nonlinear Networks. *IEEE Trans.*, Vol. 11, No. 2, June 1964, pp. 195- 201.

[24] Grasso, F., Luchetta, A., Maneti, S., Piccirilli, M.C. Symbolic Techniques for the Selection of Test Frequencies in Analog Fault Diagnosis. *Analog Integrated Circuits and Signal Processing*, no. 40, 2004, pp. 205–213.